P9.4 Composite Analysis of Environmental Conditions Favorable for Significant Tornadoes across Eastern Kansas

Joshua M. Boustead*[1], and Barbara E. Mayes
NOAA/NWS WFO Omaha/Valley, NE

William Gargan, George Phillips, and Jared Leighton
NOAA/NWS WFO Topeka, KS

1. INTRODUCTION

Decision support services (DSS) within the National Weather Service (NWS) have become an increasingly important aspect of the role of operational meteorologists. Although tornadoes occur in all states, the majority, especially significant tornadoes (STs; EF2 or greater), occur in the central and eastern United States. Thus, for operational forecasters in this area attempting to provide high levels of DSS, forecasting ST is a vital part of the job.

Significant advancements have been made since the 1950s in the forecasting and warning for severe local storms. The widespread use of Doppler radar within the NWS since the mid 1990s has aided the probability of detection of severe local storms producing flash flooding, large hail, damaging winds, and tornadoes. This, along with public education, has led to a significant drop in tornado-related deaths since the 1950s. Nevertheless, anticipating the occurrence of significant events, even in the first 24 hours, continues to be a challenge to operational forecasters at times.

The forecasting of hazardous weather continues to be a very important part of the thunderstorm warning process. Improvements in identifying patterns that can produce potentially significant events can lead to improved DSS. This pattern recognition type of severe storm forecasting has been around for some time. Miller (1972) identified several patterns in which severe thunderstorms can be expected, and Johns and Doswell (1992) indicated that pattern recognition will likely be an important part of operational forecasting in the future. Finally, the knowledge of the potential significance of an event can help forecasters better plan for staffing levels to meet the needs of the customers.

This study looks at one aspect of severe local storms forecasting, that of STs across eastern Kansas (Fig. 1). Although the precise mechanisms that lead to the development of a tornado are still unclear to some degree, operational experience indicates they frequently occur either along mesoscale boundaries or within the warm sector of a synoptic scale extratropical cyclone where significant ambient low-level horizontal vorticity exists.

There are several goals to this study. The first goal is to create a composite of the synoptic environment associated with STs that occur both with and without discernable surface boundaries, providing forecasters mental maps to utilize in anticipation of tornadic activity. The second goal is to develop climatology of significant tornadoes in eastern Kansas, including favored time of day, distribution through the convective season, and other details useful to operational forecasters. Third, this study will look at the thermodynamic and wind shear environment associated with ST occurring in Kansas, again both with and without discernable surface boundaries, while developing statistical relationships associated with their occurrence. Finally, this study will examine how the synoptic environment changes during the warm season.

2. DATA AND METHODOLOGY

A list of STs was compiled using Storm Data (NCDC 1979-2008) from 1979 through 2008 for a part of eastern Kansas (Fig. 1). Observed surface data was obtained and then plotted using the Digital Atmosphere program. Subjective surface analyses were completed for each of the tornado occurrences 2 hours prior to 1 hour post tornado occurrence. Tornadoes were grouped in two different categories; ones occurring within 50 km of a discernable (subjectively analyzed) surface boundary and tornadoes occurring without any discernable surface boundary.

Once compiled, it was noted that a number of the tornado days contained multiple STs. To reduce the possibility that one particular day would obscure or overwhelm the data when compositing, a couple of different criteria were developed for tornadoes to be included in the study. If more than one tornado occurred on a given calendar day, the first tornado for the day would always be used. For any of the subsequent tornadoes to be included in the study, they either had to occur within a different synoptic regime (i.e. first tornado was along a warm front, and the second tornado was not associated with a discernable surface boundary), and/or the tornado had to occur 3 hours after the first

[1] *Corresponding author address:* Joshua M. Boustead, 6707 N. 288th Street, Valley, NE 68064; email: josh.boustead@noaa.gov

tornado.

After the final database of STs was completed, North American Regional Reanalysis (NARR) data were obtained from the National Climate Data Center's (NCDC) NOAA National Operational Model Archive and Distribution System (NOMADS) website. The NARR dataset is a 32 km, 3 hourly regional reanalysis for North America (Mesinger et al. 2005). The 3 hourly NARR data for the closest time just prior to a particular tornado occurrence was plotted. NARR data was plotted using the General Meteorological Package (GEMPAK; DesJardins 1991).

Using the NARR data, a tornado relative composite grid was calculated. This method is similar to that completed by Moore et al. (2003) in which a system relative composite was completed for heavy rainfall events across the central United States. This was done by extracting a standard subset of the NARR data. This subset area was centered on the beginning location of the tornado and extended west 14°, east 7°, south 11°, and north 10°. Then the data were averaged by tornado type. Before putting the composited grids into GEMPAK, the data were given the same latitude and longitude, centered on Topeka, KS, for demonstration purposes. The result was a GEMPAK grid where all tornadoes in the study occurred at a latitude and longitude of Topeka, KS. An example of this process is presented in figure 2.

3. RESULTS

A. Climatological Results

Compiling a database of STs across a particular area, in this case eastern Kansas, allows for a climatological analysis of the data. Table 1 is an analysis of STs in relation to the time of day and year. There is general agreement that most STs occur during the late afternoon or early evening in the spring months. One difference is that front sector cases occur in the late evening and overnight hours with multiple peaks in activity, while warm sector cases center from the late afternoon into the early evening with one maximum occurring at 1900 CST. There are some differences in the time of year in which STs occur. Front sector cases tend to happen mid to late spring into early summer with the climatological maximum occurring in May and June, while the maximum for warm sector cases occurs in March through early May.

There are also some differences in the characteristics of the STs that occur in each sector (Fig. 3). STs in the warm sector tend to have greater width and also travel farther in distance than those associated with a front. In addition, on days where STs occur in eastern Kansas, warm sector days were slightly more likely to have multiple occurrences than front sector cases. Finally, as seen in figure 4, warm sector tornadoes also tend to be stronger as well. In the current database, there are no occurrences where a front sector tornado was stronger than F3; this is compared to a low percentage of tornadoes in the warm sector in the F4 to F5 range.

B. Synoptic Overview

The comparison of the 300 hPa analysis is presented in figure 5. The most striking difference is the stronger upper level jet associated with warm sector STs. This may be in response to the propensity of warm sector tornadoes to occur earlier in the spring, but may also signify stronger dynamics are needed for warm sector tornadoes.

There are some noteworthy similarities though. First, the favored location of STs is in the front exit region of the 300 hPa jet. This is a favored area of large-scale ascent associated with the ageostrophic jet circulation. Also of note is that in both synoptic environments, a well defined short-wave trough is upstream of the tornado development, and in both cases the wave is negatively titled.

The 300 hPa wind rose (Fig. 6) indicates a strong signal that at jet level, the wind direction for STs is from the southwest. Although warm sector cases tend to exhibit a stronger synoptic system, the wind rose indicates larger variability in both speed and direction.

Figure 7 is the 500 hPa analysis comparison. Again, the warm sector cases appear to be associated with much stronger synoptic system. In both cases, a thermal trough can be seen, but in the warm sector cases, the thermal trough is displaced upstream of the location of the trough in the height field. This may indicate that many STs are associated with a deepening synoptic system. Cold air advection (CAA) is indicated in both frontal and warm sector cases near the location of the ST. As with 300 hPa, there is strong agreement in the placement of the jet near the location of the beginning of the ST. There is also a similarity in the placement of the upstream vorticity max in relation to the ST occurrence.

Comparison of forcing using Q-vectors at 500 hPa indicates strong agreement near the location of the ST (Fig. 8). In both sectors, there is large-scale forcing for ascent near and just upstream of the ST location. In the front sector cases, this forcing tends to occur along and on the cool side of the boundary, while in the warm sector composite, there is some suggestion that forcing extends down the dry line.

Very little variation in wind direction is indicated in the 500 hPa wind rose for the warm sector cases (Fig. 9), with nearly 65 percent of the cases indicating southwest flow. Wind direction is more veered in the front sector cases, with more variability noted.

The 700 hPa comparison is presented in figure 10. The most noteworthy difference is in the thermal advection. In the warm sector cases, there is strong CAA taking place near and upstream of the ST, whereas in the front sector cases warm air advection (WAA) is indicated. In both synoptic patterns, pronounced dry air is noted upstream of the ST location, and there remains good agreement in the placement of the wind maxima near the location of the tornado.

This can also be seen in the 700 hPa wind rose (Fig. 11). The wind rose indicates that when there is stronger mid-level flow, it is typically from the southwest in both environments. Little variation is noted in the warm sector cases, with the majority of the events occurring with 20 m s^{-1} or greater wind speeds. In the front sector cases, when the mid-level flow is from the west, the flow is generally at or below 10 m s^{-1}.

A comparison of the 850 hPa composites is presented in figure 12. There are a number of similarities in both synoptic environments: the ST generally occurs to the south of the 850 hPa warm front, the event occurs within the moisture axis, and it is to the northeast of the thermal axis. The most significant difference is that the warm sector ST generally occurs on the western edge of the moist axis, while in the front sector, it is near the apex of the axis. The strong agreement in the pattern is also apparent in the 850 hPa wind rose (Fig. 13) where near 90 percent of the wind direction in both cases are from 170 to 200°.

C. Convective Results

A simple overview of the convective environment in both scenarios is presented in figure 14. ST in the warm sector cases typically occurs just to the southeast of the surface low pressure and on the western edge of the 180 hPa mixed-layer (ML) convective available potential energy (CAPE) maximum. This is also a region of weak ML convective inhibition (CIN). Deep-layer shear is near 25 m s^{-1} and is oriented at an angle which has been shown to be favorable for discrete storm activity (Bluestein and Weisman 2000; Dial and Racy 2005).

In the front sector cases in figure 14, the ST generally occurs to the east or northeast of the surface low along a well defined boundary, possibly a warm front. This is near the apex or just northeast of the MLCAPE maxima, and again is near an area of weaker MLCIN. In the front cases, there is stronger MLCIN immediately to the south of the composite boundary, and this may be one factor in the lack of any occurrence of a warm sector ST on a day where a front sector ST occurred. Deep-layer shear in the front sector generally was oriented along the warm front which may favor supercells to move nearly parallel to the boundary, possibly enhancing the available horizontal vorticity.

The composite soundings are presented in figure 15 and largely support the agreement in the synoptic scale found above. Both soundings indicate significant low-level moisture, with specific humidity of at least 8 g kg^{-1} up to 800 hPa. Above the moisture, mid-level lapse rates in the 700 to 500 hPa layer were at or above 7 °C km^{-1}. The wind profiles are also similar, with the warm sector exhibiting stronger winds throughout the vertical profile as a result of the stronger synoptic systems which accompany the warm sector tornadoes. The front sector wind profile is weaker and further backed to the southeast than in the warm sector which allows for stronger veering around 900 hPa than in the warm sector cases.

D. Statistical Results

Soundings and hodographs were analyzed individually to gather indices which have been shown to be important in the convective environment assessment. Figure 16 gives the thermodynamic and kinematic comparisons. As was apparent in the composites, the MLCAPE and MLCIN are very similar for both environments. The higher values in the front sector cases are likely a result of the later seasonal occurrence of the events. Although the low-level thermal properties are similar, a higher median lifted condensation level (LCL) and level of free convection (LFC) are indicated in the warm sector cases. This is likely a result of the deeper boundary layer mixing and higher low-level lapse rates than in the front sector cases (not shown).

Shear has long been shown to be an important factor in allowing for unorganized convection to organize and produce rotation (Klemp and Wilhelmson 1978). As would be expected given the general large-scale agreement in synoptic wind fields, the 0 to 6 km shear for both sectors is very similar. The most significant differences were apparent in the low-level shear, especially in the 0 to 2 km layer. Davies-Jones et al. (1990) indicated that using storm-relative helicity (SRH) can give an estimation of the available streamwise horizontal vorticity for low-level mesocyclone formation. A comparison of 0 to 2 km SRH indicates warm sector cases tend to have significantly higher values. This may again be due to the earlier seasonal occurrence of the warm sector events, but appears to correlate well with the higher ambient low-level SRH needed to produce ST without enhancement of the environment from a boundary.

A similar pattern is noted in the comparison of 0 to 2 km bulk shear. This is likely a result of the stronger wind speeds and more unidirectional low-level hodograph in the warm sector cases, as seen in the vertical wind profile in figure 15. Another significant difference is in the storm relative winds. Storm-relative winds have been shown to influence storm morphology (Rasmussen and Straka 1998), and the results here agree well with those findings. In the 0 to 2 km layer, as well as other layers (not shown), the 50^{th} to 75^{th} percentiles of storm relative winds are near or above 10 m s^{-1}. The only weakness in storm-relative flow is in the 4 to 6 km layer in the front sector cases, which may indicate many of these supercells tend to be high precipitation supercells. Higher values of storm relative winds in the 0 to 2 km layer seem to be important in the warm sector cases, with values much higher than indicated in the front cases.

4. CONCLUSIONS

Composites of environmental conditions for STs occurring with and without discernable surface boundaries were done for eastern Kansas. A database of STs was made, and NARR data was obtained for the each tornado occurrence. The composites were completed in a storm relative framework where the NARR data was adjusted so that all initial tornado touchdowns occurred at the same latitude and longitude (Topeka, KS).

There is considerable agreement in the large-scale environment for STs occurring with or without discernable surface boundaries. In both composites, the ST occurs in the left exit region of the strong 300 hPa jet. At 500 hPa, there is an upstream negatively titled upper level trough providing large-scale support for ascent near the location of the ST. The ST was located within the mid-level jet indicated at both 500 and 700 hPa. Upstream dry air was also located in both scenarios at 700 hPa. At 850 hPa, the ST was located within the moisture axis and near the location of the strongest low-level jet. This strong agreement in the large-scale pattern was also evident in the wind rose diagrams. Nearly all events occur with winds that are nearly due south at 850 hPa and veer to the southwest aloft starting at 700 hPa. No warm sector northwest flow events were recorded, while around 8 percent of the front sector events occurred under northwest flow at 500 hPa.

There were also some noteworthy differences in the way STs occurred in the two different sectors. On the synoptic scale, the most significant differences were that CAA was indicated at 700 hPa in the warm sector cases, while there was WAA indicated in the front sector. Warm sector ST occurred on the western edge of the 850 hPa moisture axis, while in the front sector cases, the event was near the apex. This also translated to where in relation to the MLCAPE maximum the ST occurred. In the warm sector composite, the ST occurred on the western edge of the MLCAPE axis and to the southeast of the surface low pressure. In the front sector composite, the ST occurs near the apex of the MLCAPE maxima and to the northeast of the surface low pressure.

There were also noteworthy differences in convective parameters near the location of the ST. The LCL and LFC heights for the warm sector cases are higher than in the front sector cases, which is a likely result of the deeper boundary-layer mixing and steep low-level lapse rates. Although deep-layer shear values were similar in both cases, there were significant differences in the low-level wind environment. Significantly higher values of 0 to 2 km SRH, bulk shear, and storm-relative winds were indicated in the warm sector cases.

A climatological analysis of the database was also completed to look for differences in the characteristics of the tornadoes. Findings indicated that nearly all warm sector ST events occurred from the late afternoon into the early evening hours, with no events after midnight or through the morning hours. In comparison, front sector STs occurred at all hours of the day, peaking in the evening hours. Warm sector events also tended to occur earlier in the convection season, peaking in March through early May, with only isolated events into June. STs near a boundary, although peaking in May and June, were observed in mid-summer months with greater frequency than warm sector events. It was also found that STs in the warm sector also tended to be stronger than those near a boundary, with no front sector stronger than F3 in the dataset. Finally, STs in the warm sector tended to travel greater distances and be of greater width. There was a small indication that warm sector tornado days tended to have a higher chance of having multiple ST in one event.

With a goal of providing assistance in DSS to operational forecasters with warning responsibility, composite maps have been developed for both warm sector and front cases (Fig. 17).

Acknowledgments: The authors would like to thank Dr. Graves of St. Louis University for providing the composite software and support in its installation and use.

References

Bluestein, H. B. and M. L. Weisman, 2000. The interaction of numerically simulated supercells initialized along lines. *Mon. Wea. Rev*., **128**, 3128-3149.

Davies-Jones, R., D. Burgess, and M. Foster, 1990: Test of helicity as a tornado forecast parameter. Preprints *16th Conf. on Severe Local Storms*, Kananaskis Park, AB, Canada, Amer. Meteor. Soc., 558-592.

DesJardins, M. L., K. F. Brill, and S. S. Schotz, 1991: GEMPAK5 users guide. NASA Technical Memorandum, 4260 pp. [available from NASA, Code NTT-4, Washington, DC 20546-0001]

Dial, G. L. and J. P. Racy., 2005. Forecasting short term convective mode and evolution for severe storms initiated along synoptic boundaries. Preprints, *17th conf. of Numerical Wea. Prediction*, Washington, DC, Amer. Meteor. Soc.

Johns, R. H. and C. A. Doswell III, 1992: Severe local storms forecasting. *Wea. Forecasting*, **7**, 588-612.

Klemp, J. B, and R. B. Wilhelmson, 1978: Simulations of right and left moving storms produced through storm splitting. *J. Atmos. Sci*., **35**, 1097-1110.

Mesinger, F, G. Dimego, E. Kalnay, K. Mitchell, P.C. Shafran, W. Ebisuzaki, D. Jovic, J. Woolen, E. Rodgers, E. H. Berbey, M.B. Ek, Y. Fan, R. Grumbine, W. Higgins, H. Li, Y. Lin, G. Manikin, D. Parrish, and W. Shi., 2005: North American regional reanalysis. *Bull. Amer. Meteor. Soc*., **87**, 343-360.

Miller, R. C., 1972: Notes on the analysis and severe storms forecasting procedures of the Air Force Global Weather Central. Tech. Rep. 200 (rev.), Air Weather Service, 181 pp.

Moore, J. T., F. H. Glass, C. E. Graves, S. M. Rochette, and M. J. Singer, 2003: The environment of warm-season elevated thunderstorms associated with heavy rainfall over the central United States. *Wea. Forecasting*, **18**, 861-878.

Rasmussen, E. N. and J. M. Straka, 1998: Variations in supercell morphology. Part I: Observations of the role of upper-level storm relative flow. *Mon. Wea. Rev*., **126**, 2406-2421.

NCDC, 1979-2007: Storm Data. [Available from National Climate Data Center, 151 Patton Ave., Asheville, NC 28801-5001]

Weisman, M. L. and J. B. Klemp, 1982: The dependence of numerically simulated convective storms on vertical wind shear and buoyancy. *Mon. Wea. Rev*., **110**, 504-520.

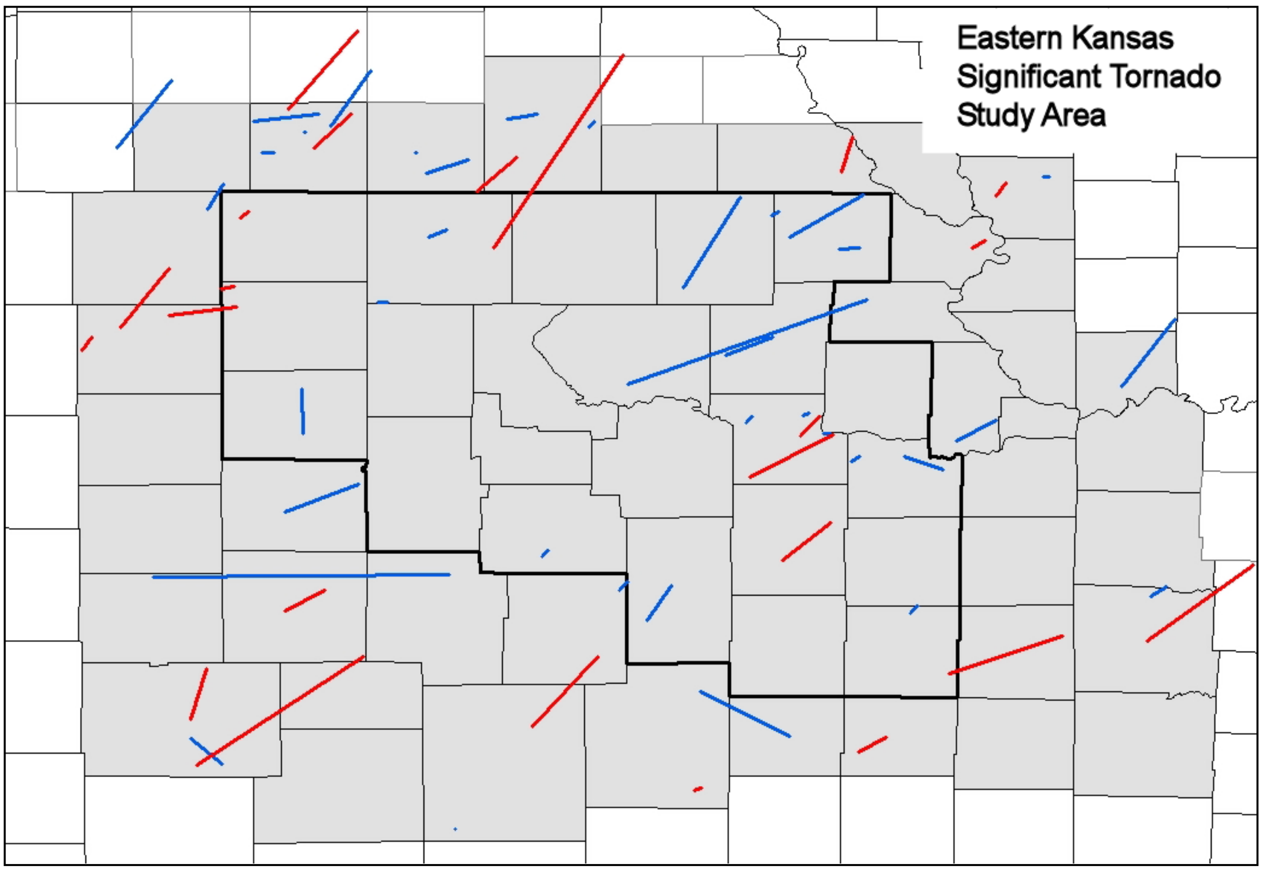

Figure 1. Outline of the study area in light blue. Thick black line outlines the warning area responsibility of the National Weather Service in Topeka, KS. Tornado tracks are overlaid, with warm sector in blue and front sector in red.

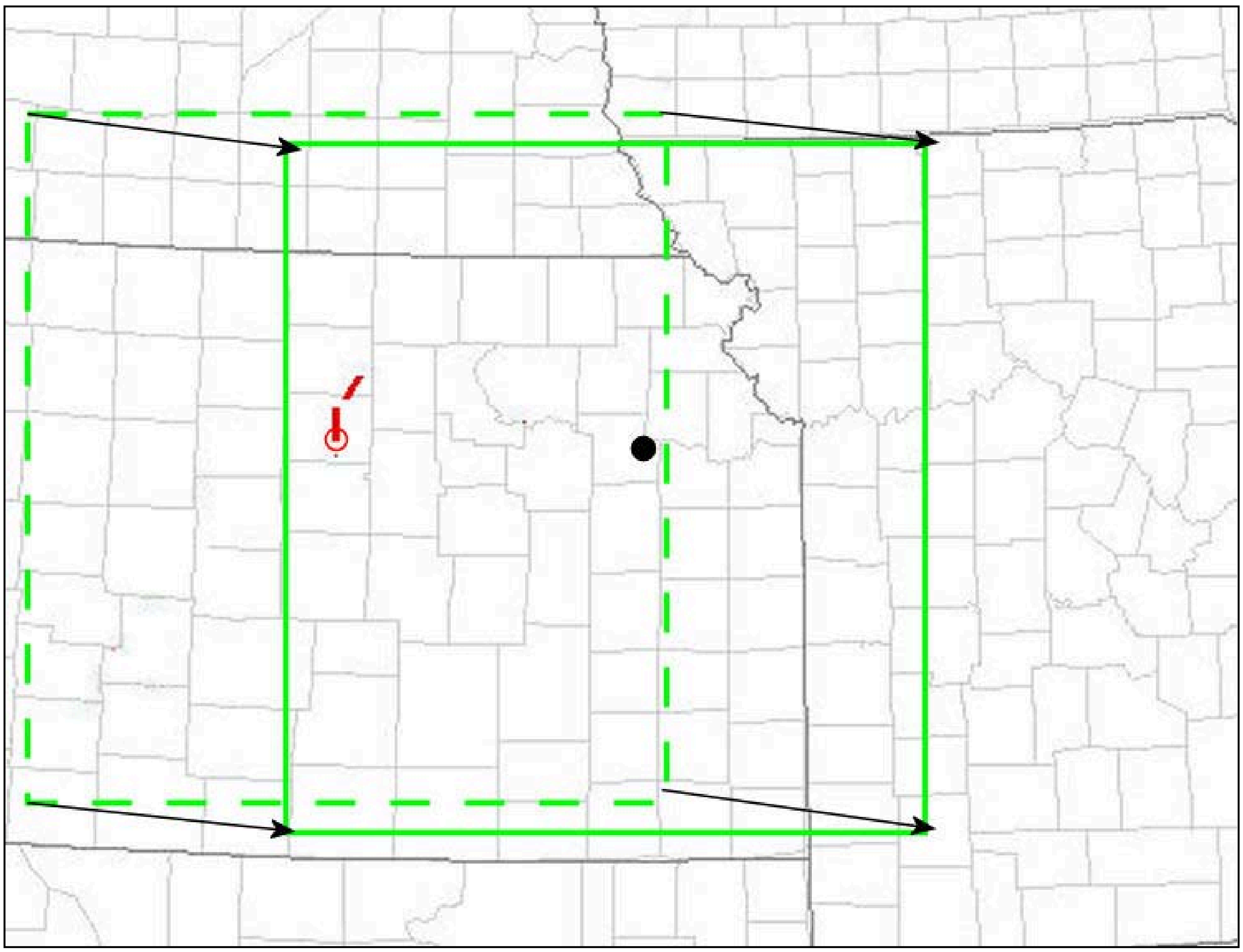

Figure 2. Idealized example of a tornado relative grid. Initial tornado touchdown is used, and a box is drawn around the tornado. That box is then moved to be centered over the latitude and longitude of Topeka, KS.

	0	1	2	3	4	5	6	7	8	9	10	11	12	13	14	15	16	17	18	19	20	21	22	23
January																								
Febuary																								
March																								
April		*1*													*1*			*1*	*1*	*1*		*1*		
May	*1*														*1*	**2**	**4**		*1*	*1*			*1*	
June				**3**												**2**	*1*	*1*	**2**	**2**	*1*	**2**		*1*
July						*1*			*1*															
August																						*1*		
September																				*1*				
October																	*1*							
November																								
December																								

	0	1	2	3	4	5	6	7	8	9	10	11	12	13	14	15	16	17	18	19	20	21	22	23
January																								
Febuary																				*1*				
March																	**2**		*1*	**3**				*1*
April																*1*	*1*		**2**	*1*				*1*
May																		**3**		**2**				
June																		*1*	*1*			*1*		
July																								
August																								
September																								
October																								
November															*1*									
December																								

Table 1. Significant tornadoes in relation to time of the year and time of day for front sector cases (top) and warm sector cases (bottom). Time is in CST.

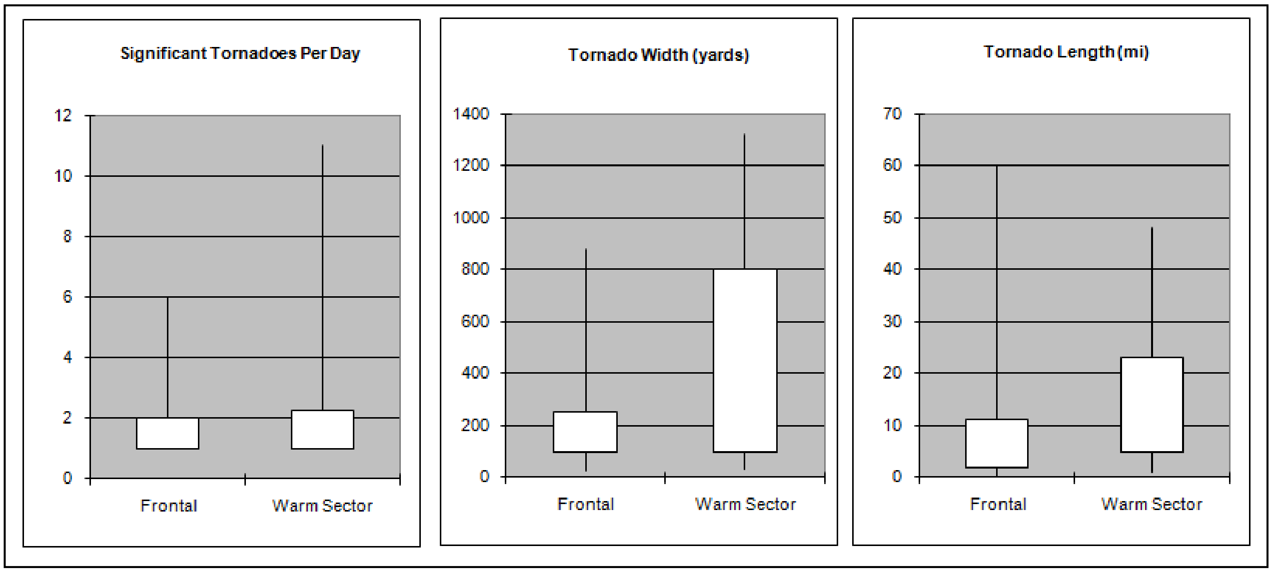

Figure 3. Significant tornado characteristics box and whiskers. Includes significant tornadoes per day in the study area, tornado width in yards, and tornado length in miles.

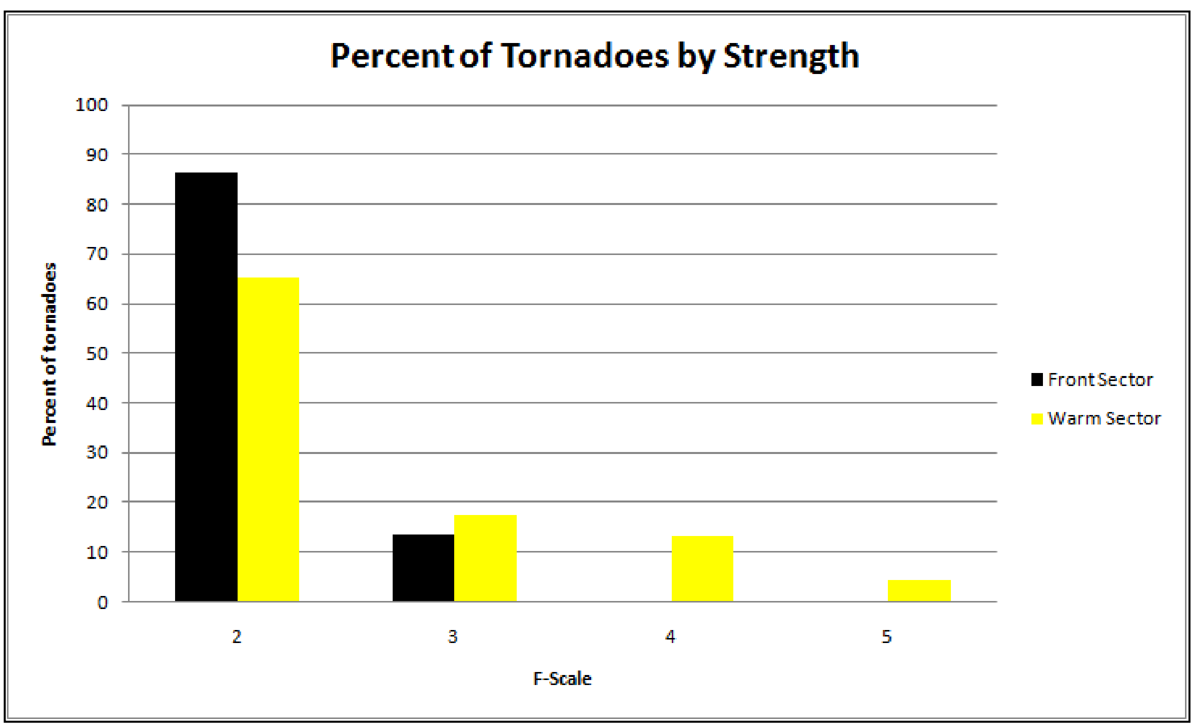

Figure 4. Comparison of tornado strength between front sector (black) and warm sector (yellow) significant tornadoes.

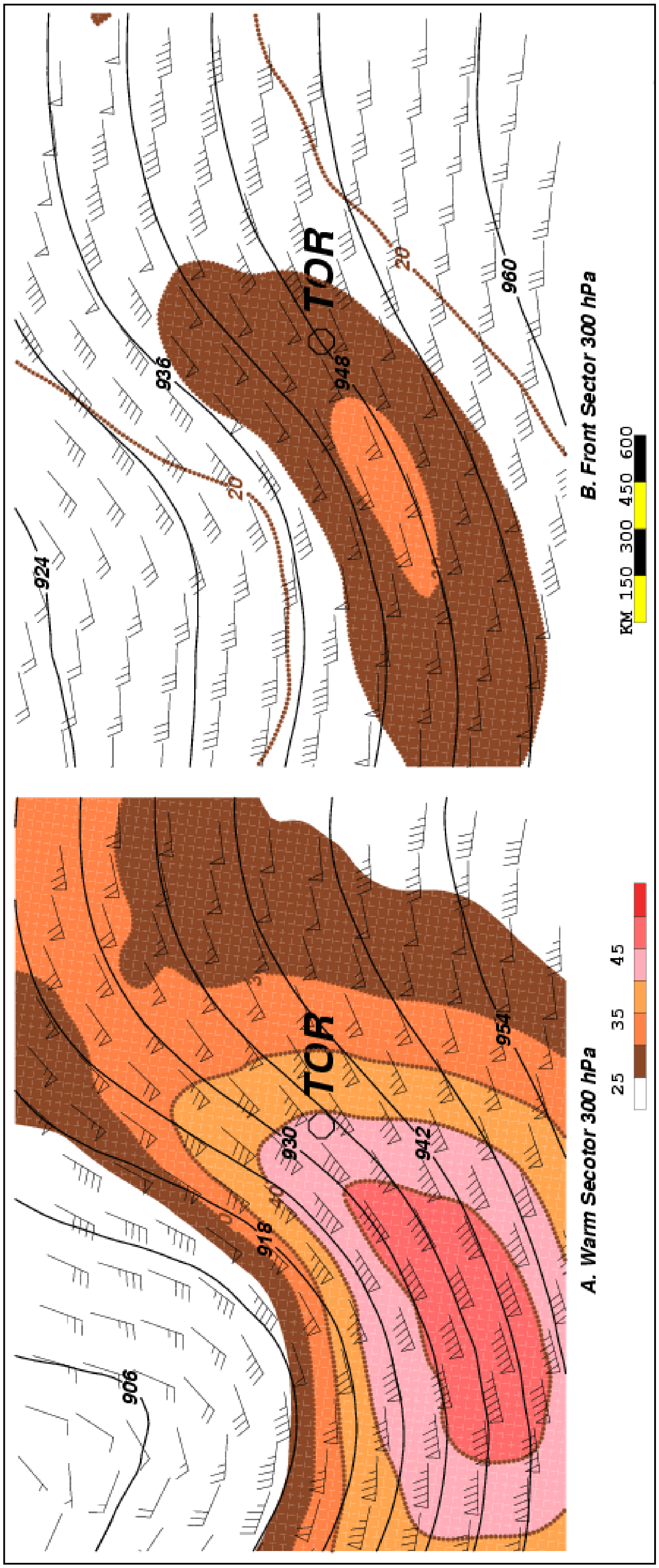

Figure 5. Composite of 300 hPa for (A) warm sector and (B) front sector (B). Thick black contours are heights in meters, contoured every 60 m. Shading is isotachs, in m s^{-1} and wind barbs are plotted in m s^{-1} with half barb 2.5 m s^{-1}, full barb 5 m s^{-1}. TOP denotes the tornado observation point in all images.

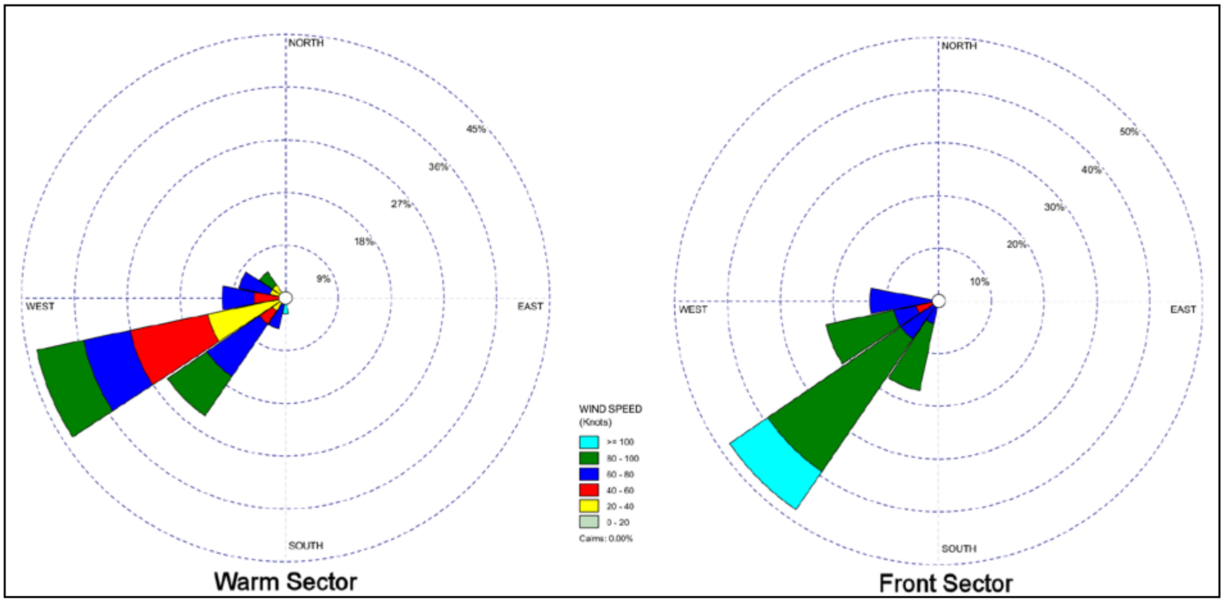

Figure 6. The 300 hPa wind rose for warm sector cases (left) and front sector cases (right). Wind is in knots.

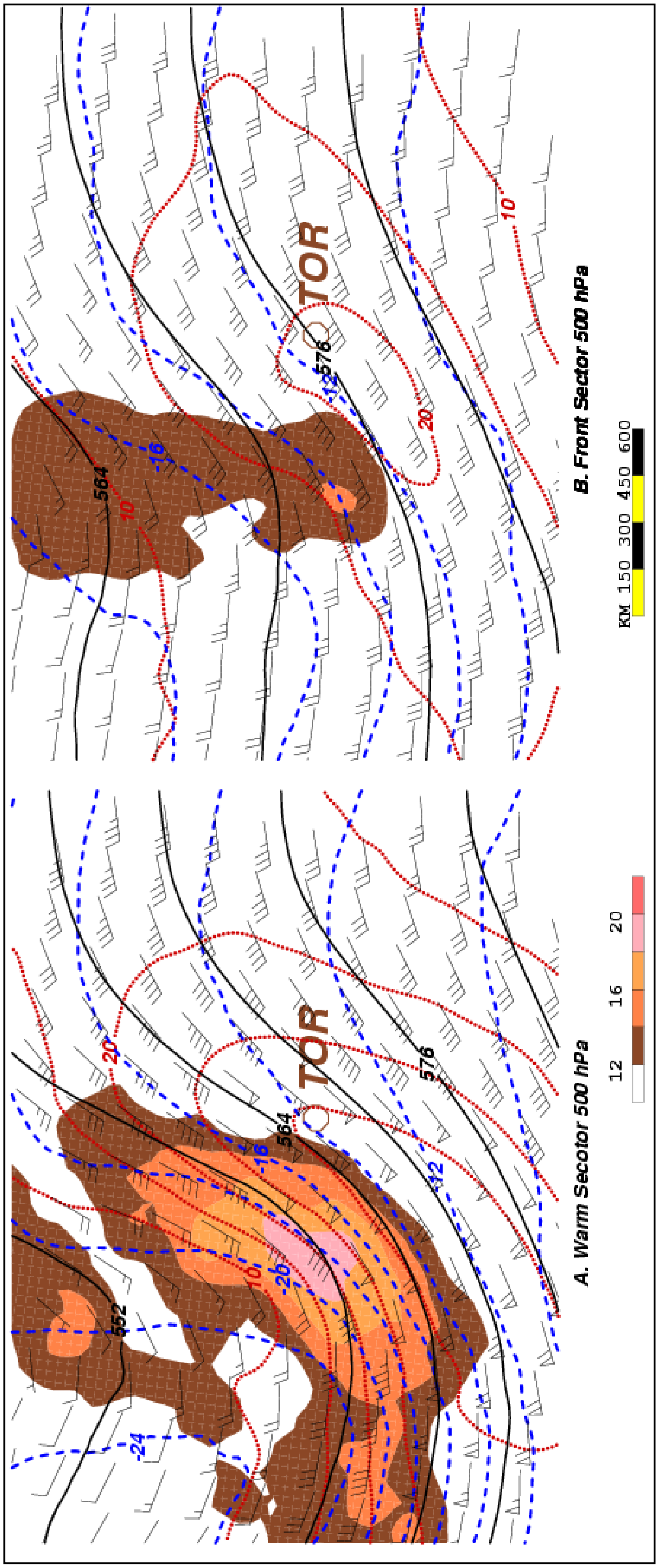

Figure 7. Composite of 500 hPa for warm sector (A) and front sector (B). Thick black contours are heights in meters contoured every 60. Shading is absolute vorticity s^{-1}. Brown dotted line is isotachs in m s^{-1}, and wind barbs are plotted in m s^{-1}, half barb 2.5 m s^{-1}, full barb 5 m s^{-1}. Dashed blue lines are temperature contoured 2 °C. TOR denotes the tornado beginning point.

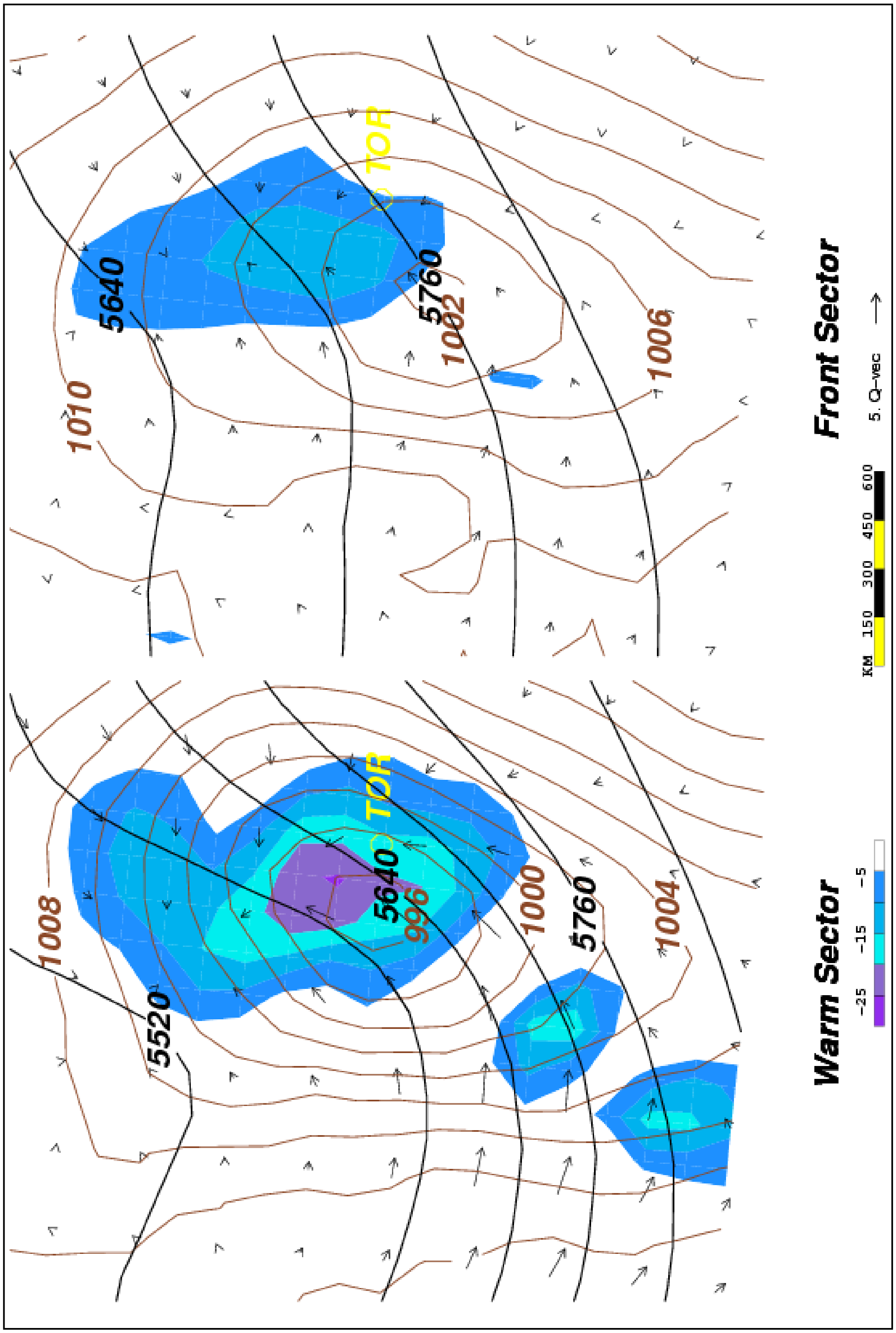

Figure 8. Composite of 500 hPa for (A) warm sector and (B) front sector. Thick black lines are heights, contoured at 60 m. Thin brown lines are surface pressure, contoured at 2 mb. Shading is divergence of Q-vectors, and arrows are Q-vectors, in kPa m^{-2} s^{-1}.

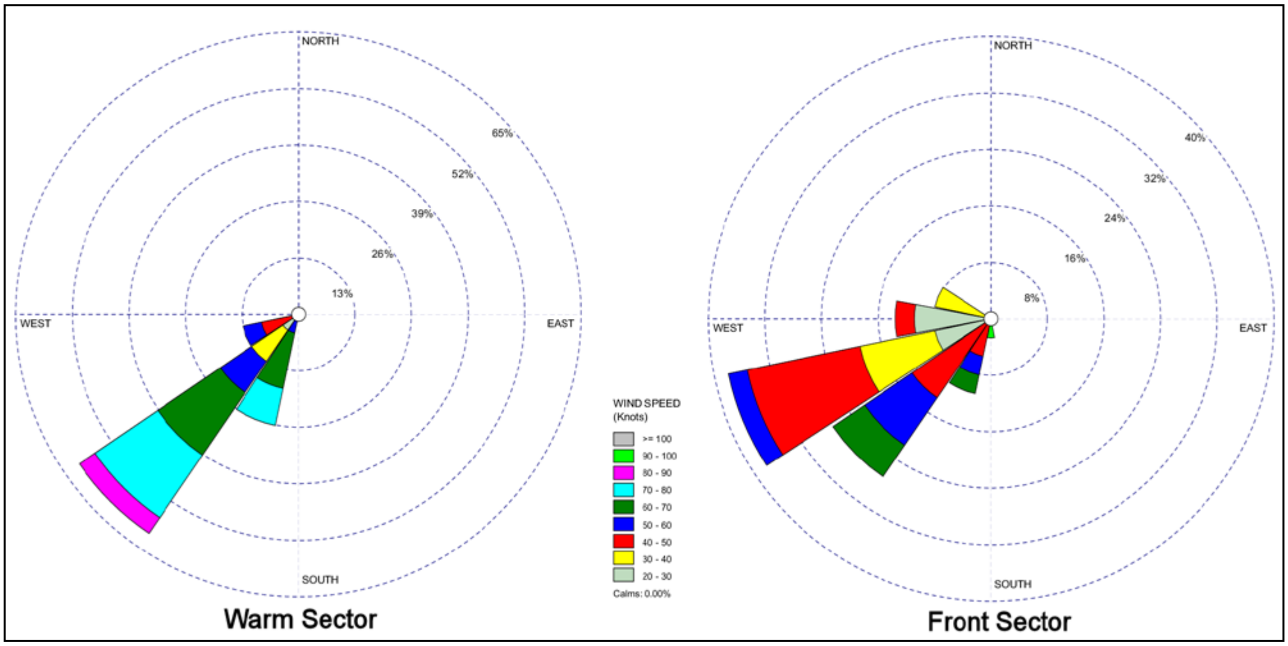

Figure 9. As in figure 6, but for 500 hPa.

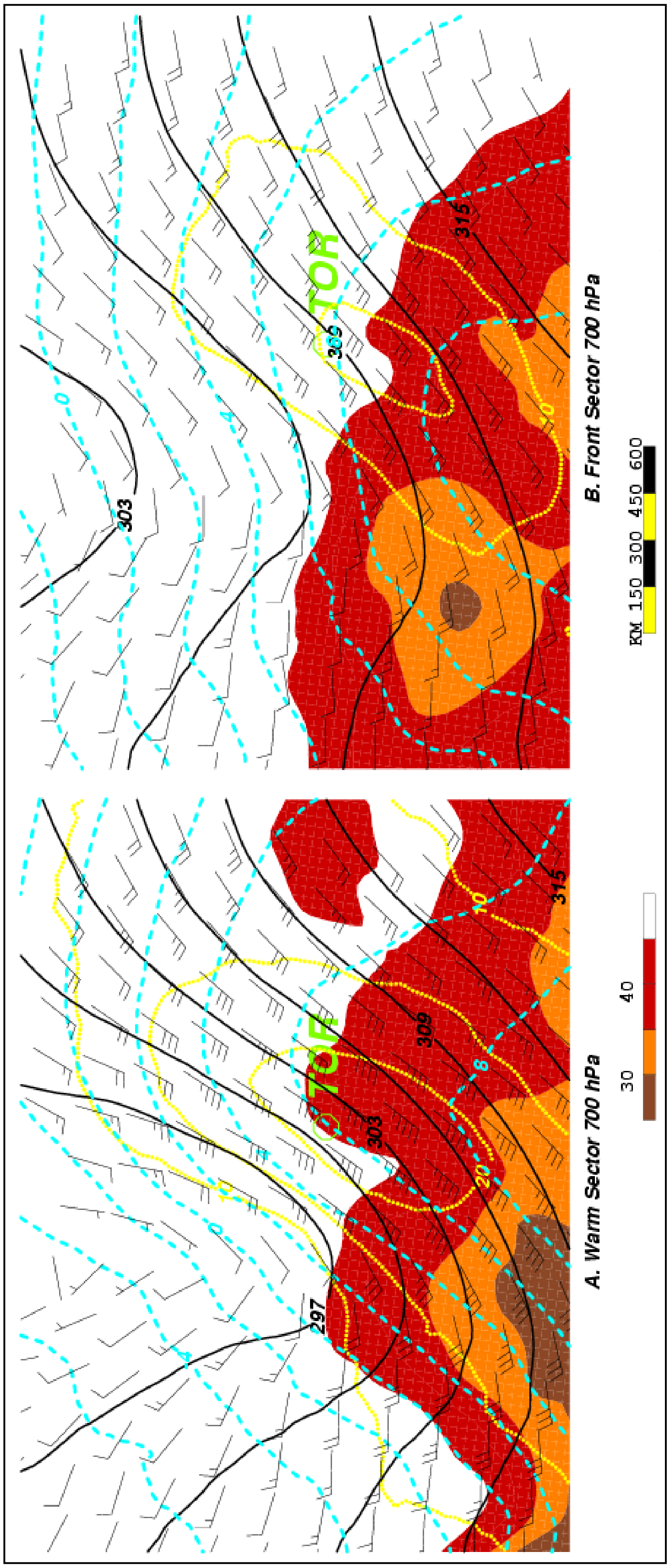

Figure 10. Composite of 700 hPa for (A) warm sector and (B) front sector. Thick black contours are heights in meters contoured every 30 m. Shading is relative humidity below 40 percent. Isotachs are yellow dotted lines in m s^{-1}, and wind barbs are plotted in m s^{-1}, half barb 2.5 m s^{-1}, full barb 5 m s^{-1}. Dashed light blue lines are temperature contoured 3 °C. TOR denotes the tornado beginning point.

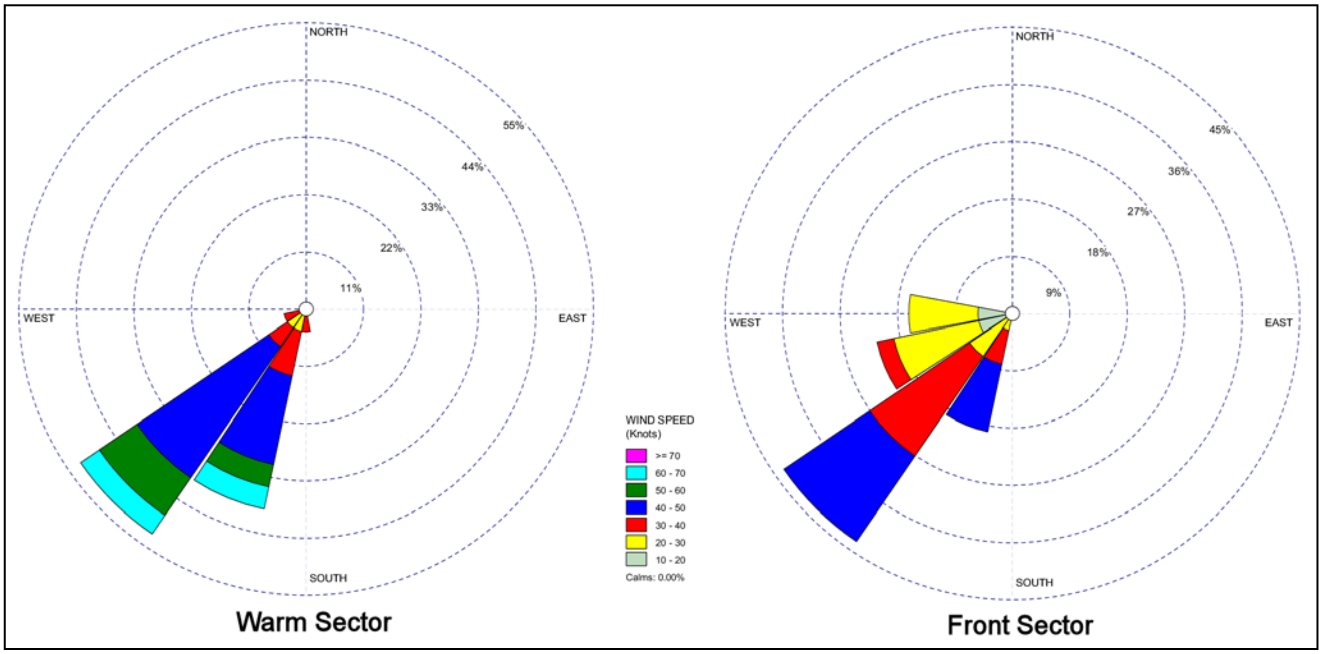

Figure 11. As in figure 6 but for 700 hPa.

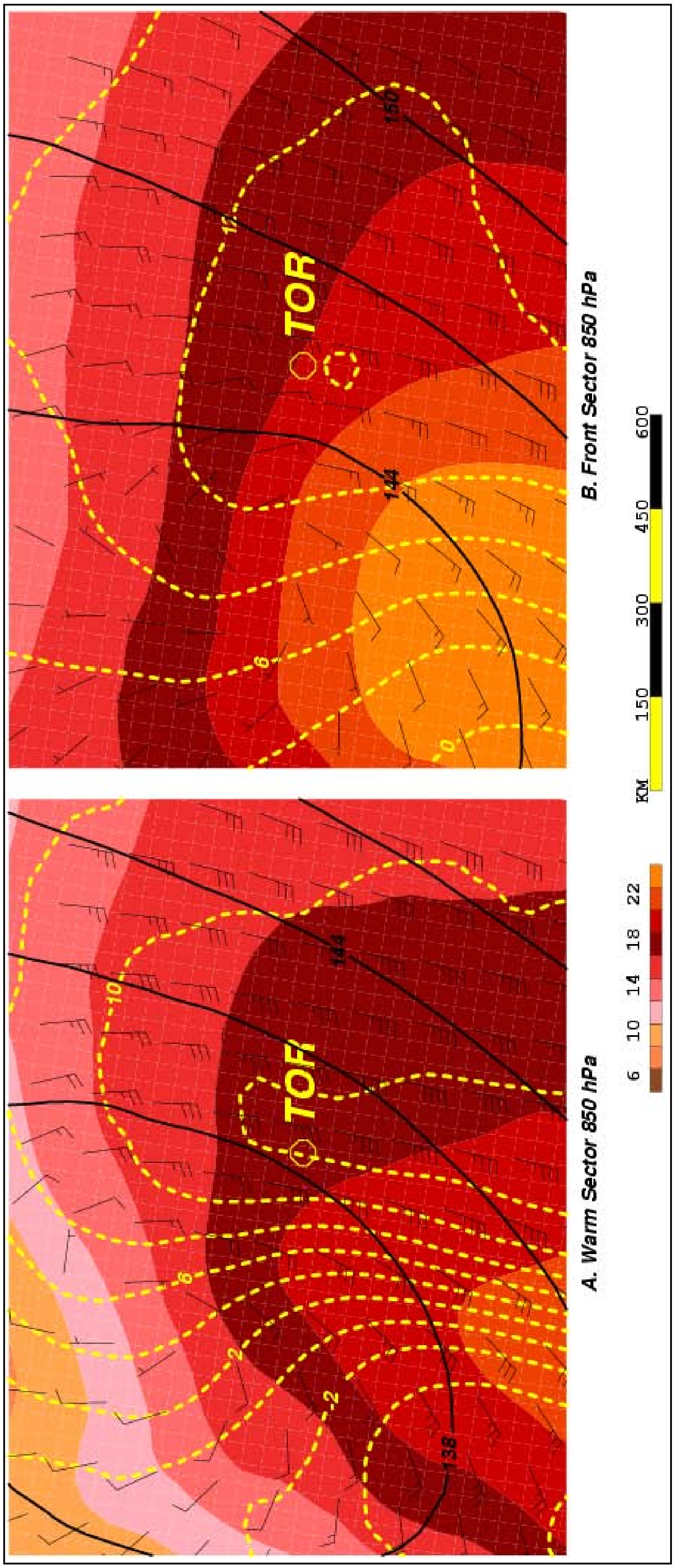

Figure 12. . Composite of 850 hPa for (A) warm sector and (B) front sector. Thick black contours are heights in meters, contoured every 30 m. Shading is temperature 2 °C. Wind barbs are plotted in m s^{-1}, half barb 2.5 m s^{-1}, full barb 5 m s^{-1}. Dashed green lines are dew point, contoured 2 °C. TOR denotes the tornado beginning point.

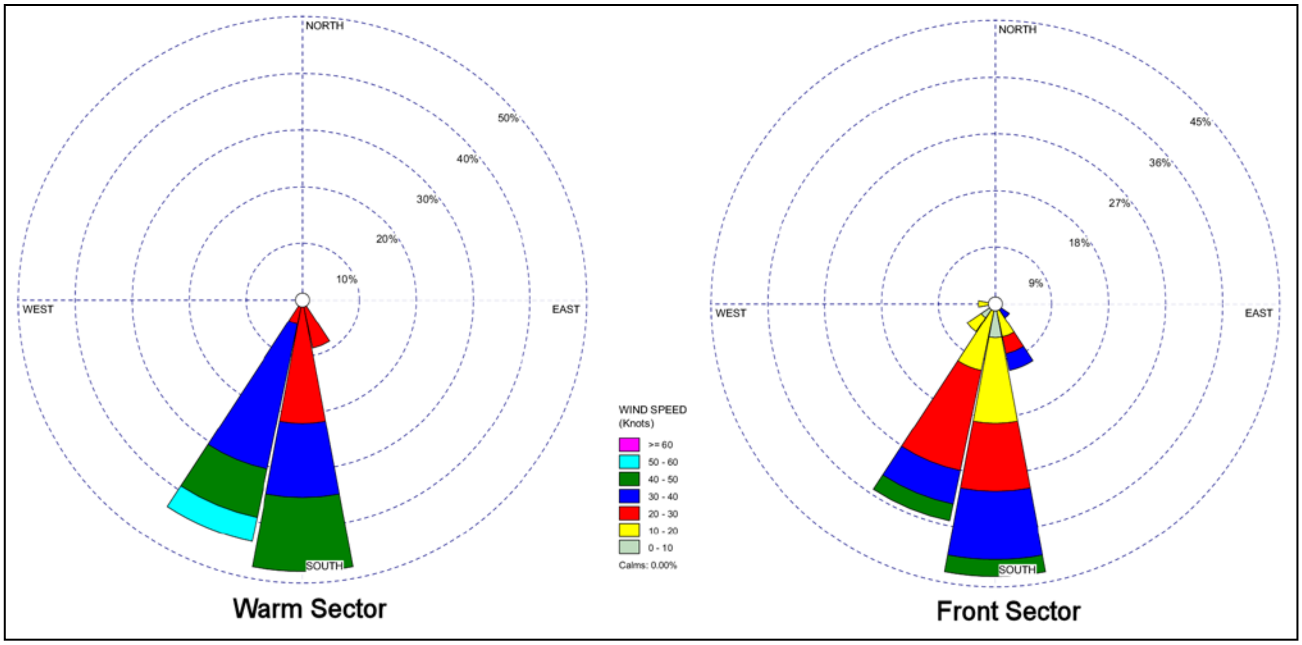

Figure 13. As in figure 6 but for 850 hPa.

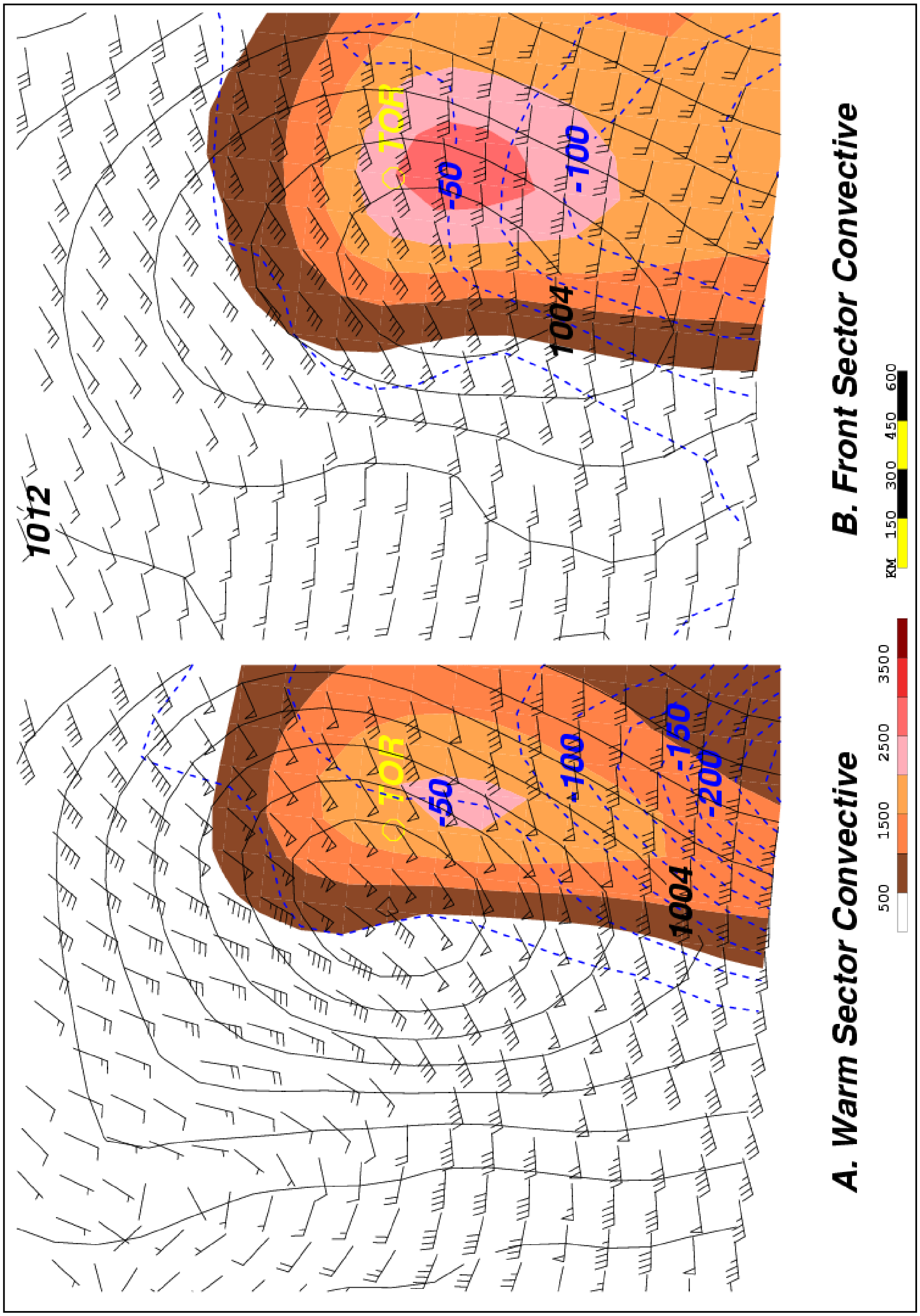

Figure 14. Convective composite for (A) warm sector and (B) front sector. Solid black lines is sea level pressure, contoured at 2 hPa. Thin dotted blue lines are MLCIN, contoured at 25 J kg^{-1}. Shading is MLCAPE, contoured at 250 J kg^{-1} starting at 750 j kg^{-1}. Barbs are 0 to 6 km bulk shear in m s^{-1}, where a half barb is 2.5 m s^{-1} and a full barb is 5 m s^{-1}.

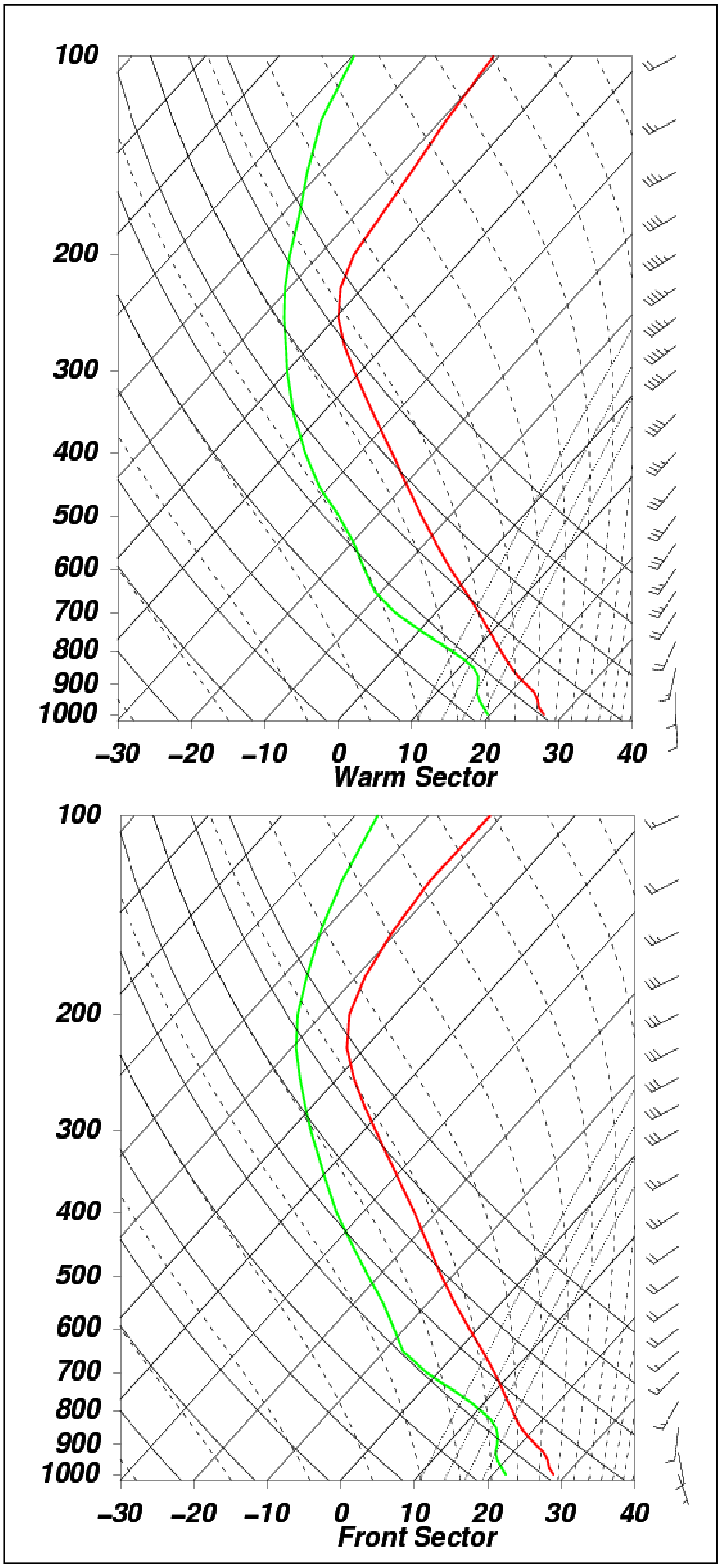

Figure 15. Composite soundings from front sector cases (top) and warm sector cases (bottom). Temperature is in red, and dew point is in green. Wind barbs are plotted in m s^{-1}, where half barb is 5 m s^{-1} and a full barb 10 m s^{-1}.

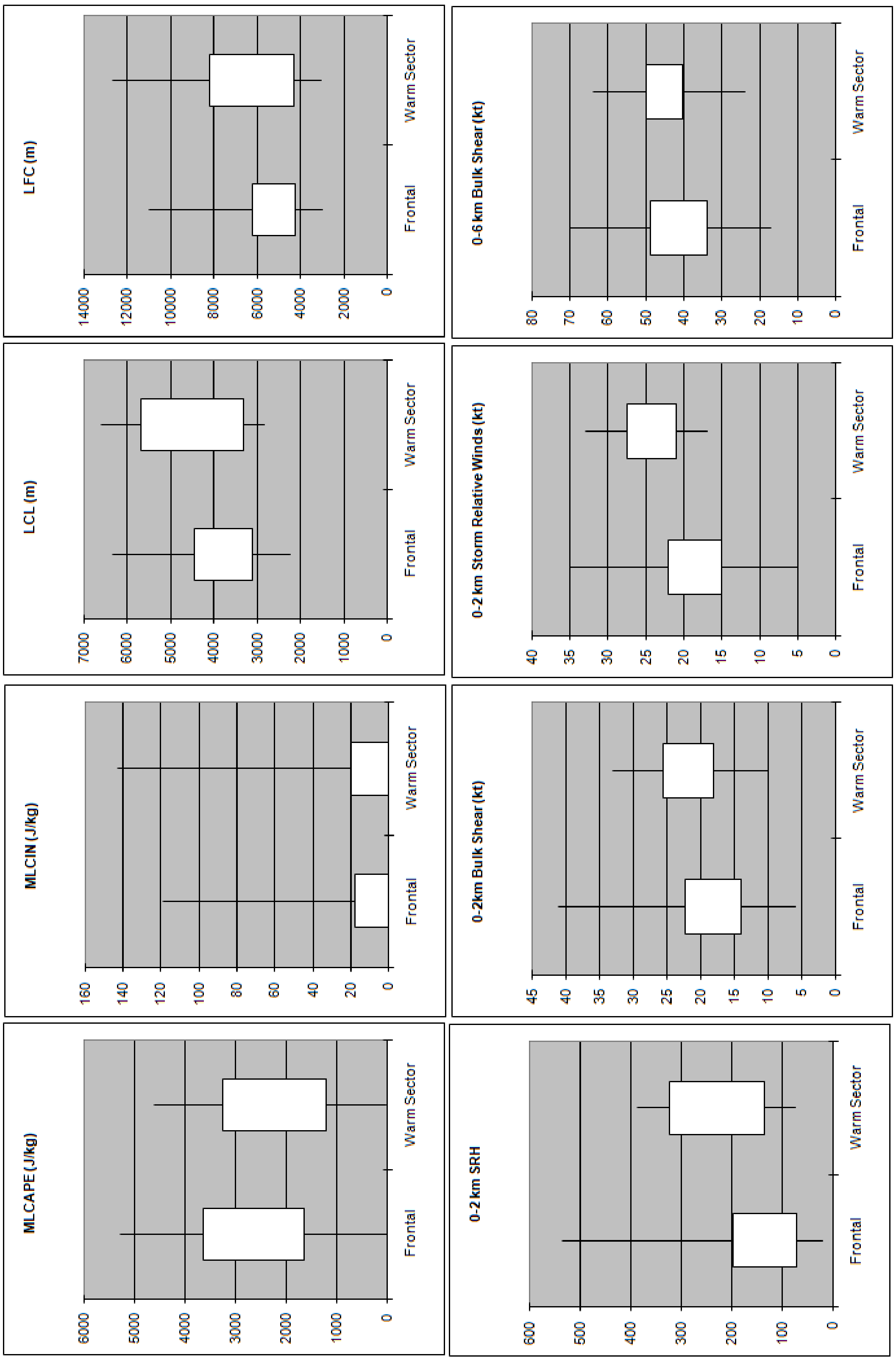

Figure 16. Comparison of various convective parameters for front sector and warm sector cases. MLCAPE (A) and MLCIN (B) are in J kg-1. LCL (C) and LFC (D) are in m. SRH (E) is in m^{-2} s^{-2}, and 0 to 2 km bulk (F), 0 to 2 km storm relative wind (G), and 0 to 6 km bulk shear (H) are in m s^{-1}.

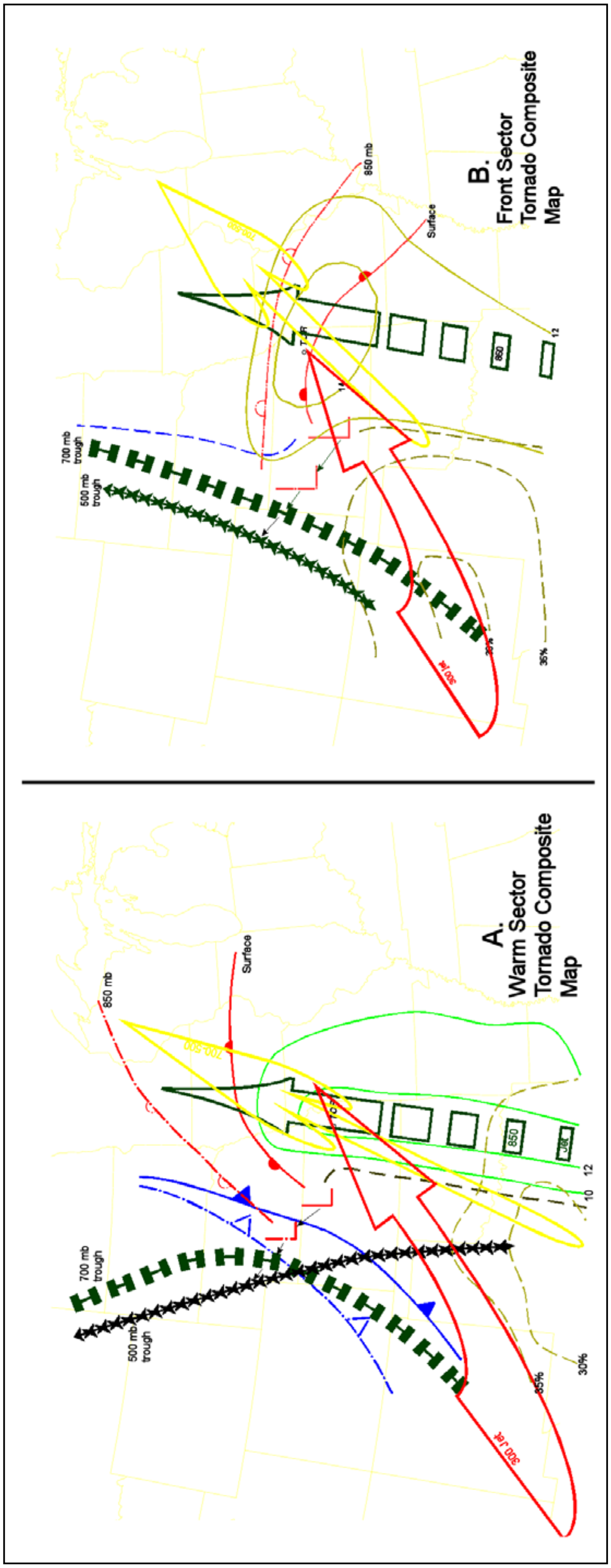

Figure 17. Idealized synoptic pattern associated with significant tornadoes in the warm sector (A) and the front sector (B). Surface pattern is plotted with conventional fronts. Surface dew points are plotted in dashed green lines and relative humidity with brown dashed lines. The 850 hPa warm front and cold front are plotted with scalloped lines, and the jet core is plotted with a large green arrow. The 700 and 500 hPa jet is plotted in the yellow arrow, and the 300 hPa jet is plotted in the thick red arrow. The orientation and location of the 700 and 500 hPa trough axis are shown.